

## **PHYSICAL AND MECHANICAL CHARACTERIZATION OF A NANO CARBON INFUSED ALUMINUM-MATRIX COMPOSITE**

Lloyd Brown<sup>1</sup>, Peter Joyce<sup>1</sup>, David Forrest<sup>2</sup>, Jennifer Wolk<sup>2</sup>

*1. U.S. Naval Academy  
Mechanical Engineering Department  
590 Holloway Road  
Annapolis, MD 21402*

*2. Naval Surface Warfare Center, Carderock Division  
Welding, Processing, and NDE, Code 611  
9500 MacArthur Boulevard  
West Bethesda, MD 20817-5700*

### **ABSTRACT**

A nanocarbon-infused aluminum-matrix composite, termed "covetic," has been developed by Third Millennium Metals, LLC, and we have evaluated the enhanced performance prospects for strength and electrical conductivity. This paper examines the effects of the nanoscale carbon on the physical, electrical and mechanical properties of the metal-matrix composite based on microscopy, hardness, quasi-static tensile strength, high strain-rate compression strength and electrical conductivity measurements. In the as-extruded condition (warm worked at 400°F) the results show that the nanocarbon provides approximately a 30% improvement in yield strength compared to baseline 6061-T0. High strain rate, Split Hopkinson Pressure Bar (SHPB) tests revealed an opposite trend—the as-extruded covetic exhibited lower stresses at equivalent strains. In the T6 condition, the strength and ductility of 6061 with and without nanocarbon are approximately equal at all strain rates. The nanoscale carbon increased the electrical conductivity of 6061 by 43% in the as-extruded condition, but by only about 1% in the T6 condition. Electron microscopy showed that the covetic 6061 was more resistant to grain growth and coarsening during extrusion. The carbon/aluminum composite displays potential as an improved strength aluminum alloy with much higher electrical conductivity than is typical for other aluminum alloys and aluminum matrix composites.

### **1. INTRODUCTION**

Third Millennium Metals, LLC (Waverly, Ohio) has developed a process (known as the *covetic* process) that creates a dispersion of significant quantities (up to 5 wt. %) of nanoscale amorphous carbon particles in a variety of metallic systems, including Al, Cu, Au, Ag, Zn, Sn, Pb and Fe [1]. The particles are tenaciously bound to the lattice, increasing strength, electrical conductivity, and thermal conductivity. This represents a significant advance in both nanomanufacturing processes and in nanomaterials. The carbon is exceptionally stable: the fine dispersion of particles remains even after remelting and re-casting the metal. Because the carbon

## Report Documentation Page

Form Approved  
OMB No. 0704-0188

Public reporting burden for the collection of information is estimated to average 1 hour per response, including the time for reviewing instructions, searching existing data sources, gathering and maintaining the data needed, and completing and reviewing the collection of information. Send comments regarding this burden estimate or any other aspect of this collection of information, including suggestions for reducing this burden, to Washington Headquarters Services, Directorate for Information Operations and Reports, 1215 Jefferson Davis Highway, Suite 1204, Arlington VA 22202-4302. Respondents should be aware that notwithstanding any other provision of law, no person shall be subject to a penalty for failing to comply with a collection of information if it does not display a currently valid OMB control number.

1. REPORT DATE <b>OCT 2011</b>	2. REPORT TYPE	3. DATES COVERED <b>00-00-2011 to 00-00-2011</b>		
4. TITLE AND SUBTITLE <b>Physical and Mechanical Characterization of a Nano Carbon Infused Aluminum-Matrix Composite</b>			5a. CONTRACT NUMBER	
			5b. GRANT NUMBER	
			5c. PROGRAM ELEMENT NUMBER	
6. AUTHOR(S)			5d. PROJECT NUMBER	
			5e. TASK NUMBER	
			5f. WORK UNIT NUMBER	
7. PERFORMING ORGANIZATION NAME(S) AND ADDRESS(ES) <b>U.S. Naval Academy, Mechanical Engineering Department, 590 Holloway Road, Annapolis, MD, 21402</b>			8. PERFORMING ORGANIZATION REPORT NUMBER	
9. SPONSORING/MONITORING AGENCY NAME(S) AND ADDRESS(ES)			10. SPONSOR/MONITOR'S ACRONYM(S)	
			11. SPONSOR/MONITOR'S REPORT NUMBER(S)	
12. DISTRIBUTION/AVAILABILITY STATEMENT <b>Approved for public release; distribution unlimited</b>				
13. SUPPLEMENTARY NOTES <b>Proceedings of the SAMPE Fall Technical Conference, Ft. Worth, TX, 17-20 October 2011.</b>				
14. ABSTRACT <b>A nanocarbon-infused aluminum-matrix composite, termed "covetic," has been developed by Third Millennium Metals, LLC, and we have evaluated the enhanced performance prospects for strength and electrical conductivity. This paper examines the effects of the nanoscale carbon on the physical, electrical and mechanical properties of the metal-matrix composite based on microscopy, hardness, quasi-static tensile strength, high strain-rate compression strength and electrical conductivity measurements. In the as-extruded condition (warm worked at 400°F) the results show that the nanocarbon provides approximately a 30% improvement in yield strength compared to baseline 6061-T0. High strain rate, Split Hopkinson Pressure Bar (SHPB) tests revealed an opposite trend—the as-extruded covetic exhibited lower stresses at equivalent strains. In the T6 condition, the strength and ductility of 6061 with and without nanocarbon are approximately equal at all strain rates. The nanoscale carbon increased the electrical conductivity of 6061 by 43% in the as-extruded condition, but by only about 1% in the T6 condition. Electron microscopy showed that the covetic 6061 was more resistant to grain growth and coarsening during extrusion. The carbon/aluminum composite displays potential as an improved strength aluminum alloy with much higher electrical conductivity than is typical for other aluminum alloys and aluminum matrix composites.</b>				
15. SUBJECT TERMS				
16. SECURITY CLASSIFICATION OF:			17. LIMITATION OF ABSTRACT	
a. REPORT <b>unclassified</b>	b. ABSTRACT <b>unclassified</b>	c. THIS PAGE <b>unclassified</b>	<b>Same as Report (SAR)</b>	18. NUMBER OF PAGES <b>14</b>
			19a. NAME OF RESPONSIBLE PERSON	



addition is performed in the melt, economies of scale through mass production is expected to lower production costs for these materials in the long term.

We seek to better-characterize covetic materials, focusing specifically on aluminum and copper, in order to assess the relationships between processing, structure, and properties and identify suitable applications for Navy systems. The exceptional thermal properties point us to applications in thermal management, improving performance in systems from microelectronic components to heat exchangers. The improved electrical conductivity of aluminum could provide more efficient motors and generators, lighter weight wiring, and improved performance in batteries and ultracapacitors. Both electrical and thermal conductivity can vary anisotropically in covetic materials, depending on processing, and this adds an additional degree of freedom to system design.

We are still in the early stages of learning how deformation processing influences the mechanical properties of covetic materials—we do know that it plays a critical role. This study provides new information on the effect of processing on microstructure and properties.

## 2. EXPERIMENTATION

### 2.1 Overview

We received a small quantity of as-extruded 12.7 mm diameter rod of 43 cm length of AA6061 with no carbon and with 3 wt% carbon (labeled H49). Both pieces were extruded at 400°F at the Wright-Patterson Air Force Research Laboratory (WPAFB). We measured density and hardness, conducted optical microscopy and image analysis, measured quasi-static tensile properties, and electrical resistivity before and after heat treatment to the T6 condition (solutionize at 985°F for 70 minutes, water quench, age at 350°F for 8 hours). In addition, we determined high strain rate properties using a Split Hopkinson Pressure Bar.

### 2.2 Density

Density measurements were performed using a Quantachrome Instruments Ultrapycnometer 1000. The gas pycnometry technique is based on the displacement of a volume of gas by a solid object placed within the test cell. The Ultrapycnometer actually measures volume, but with an attached scale to obtain the mass ( $m$ ) of the test specimen, the density ( $\rho$ ) can be calculated. Density of the 6061 aluminum was 2.678 g/cm<sup>3</sup> while that of the covetic aluminum was 2.673 g/cm<sup>3</sup>. Density of the added carbon is more difficult, as the value depends on the structure of the carbon added. For this study, carbon density was estimated to be 2.25 g/cm<sup>3</sup>, which is the value [2] for the graphitic carbon used in the fabrication of covetic aluminum. The determination of density was undertaken to facilitate evaluation of the other material properties as a function of the volume fraction ( $V_f$ ) of C since the  $V_f$  can easily be extrapolated from the density measurements using the rule of mixtures approach, more on this will be discussed later.

### 2.3 Microhardness

We performed microhardness tests using a Buehler Micromet 5103 to measure Vickers hardness. For microhardness testing, as-extruded cross sections of both 6061 and covetic aluminum were mounted and polished. The specimens were polished to a mirror finish using 0.3 micron grit

after mounting. Test results are shown in Figure 1 along with an image of a mounted specimen. The determination of hardness as a function of position within the extrusions served as a “roadmap” for future correlation of other mechanical or material properties to position within the casting.

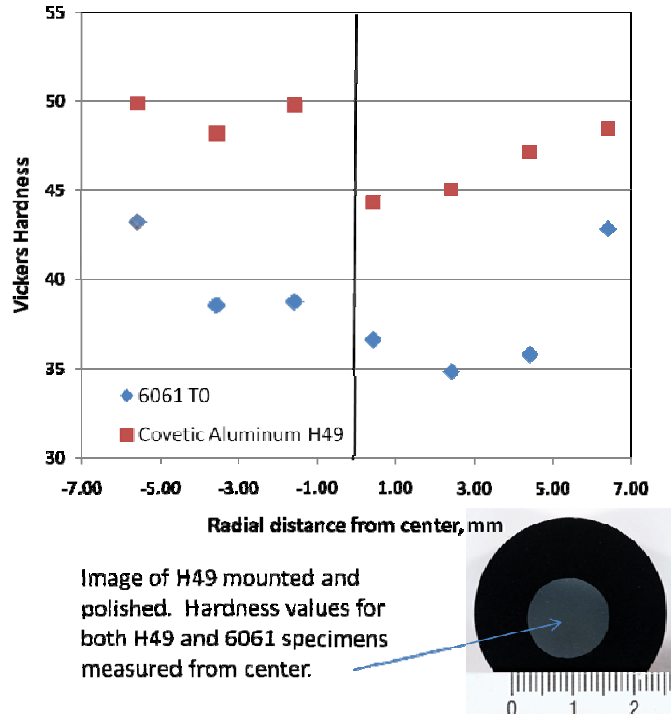


Figure 1: Vickers hardness values for both types of aluminum in the as-extruded condition, using centerline of specimens as reference point.

## 2.4 Optical Microscopy and Image Analysis

We observed some inclusions in the covetic aluminum specimen, however no such defects were noted in the comparison 6061 material. Figure 2 provides a detailed view of a hardness test point on the covetic aluminum specimen that coincided with what is likely a carbon inclusion, based on chemical analysis and appearance. Close examination of the image in Figure 2 reveals numerous dark spots, which are believed to be localized concentrations of amorphous carbon from incomplete conversion to nanoscale carbon typical of this particular heat treatment. No other defects were observed in the covetic material.

## 2.5 Electron Microscopy

We measured grain sizes and crystallographic orientations using Electron Beam Backscatter Diffraction (EBSD) analysis on as-extruded samples of conventional and covetic 6061 that were

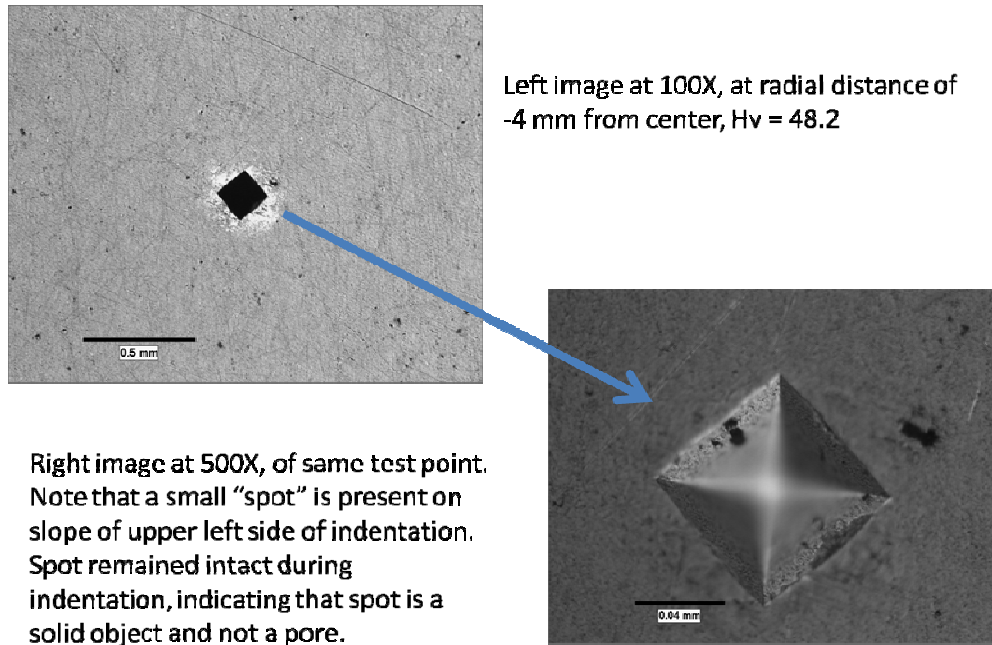


Figure 2: Covetic aluminum Vickers hardness test point, with evidence of solid inclusions in material, speculated to be agglomerated carbon.

metallographically prepared transverse to the extrusion direction. The analysis revealed a significant difference in grain size distributions between the two materials. Nearly all of the grains in the covetic material ranged between 1 and 30  $\mu\text{m}$  in diameter (with 7% of the area having grains less than 1  $\mu\text{m}$  diameter). The conventional 6061 had a strongly bi-modal distribution—with 57% of the area having grains 100-200 microns in diameter, and 25% of the area covered by grains less than 10 microns in diameter (including 3.5% of the area having grains under 1  $\mu\text{m}$  diameter). The covetic material was fine-grained and strongly textured throughout the sample, with two predominant orientations. The conventional 6061 had the same strong texture orientations only in the fine-grained regions. Where the conventional material had grown new, large grains, the orientations exhibited a random, annealed texture (Figure 3).

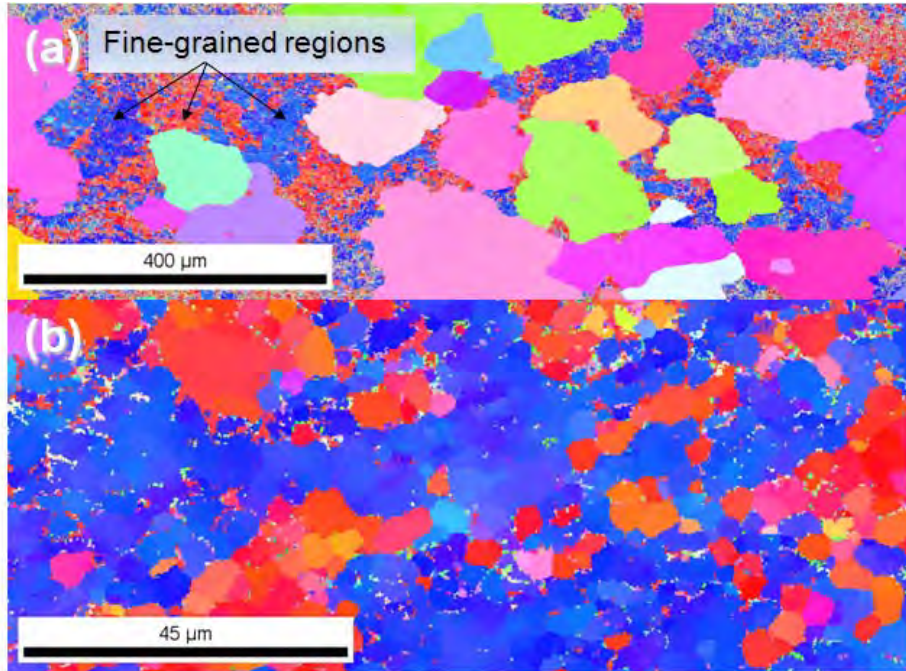


Figure 3. EBSD images of conventional (a) and covetic 6061 (b) in the as-extruded condition. The covetic material exhibited strong orientations in two different stereographic directions throughout the sample (predominantly blue and red coloration), while the conventional 6061 exhibited strong orientations only in the fine-grained regions. Different magnification scales required to show the relative magnitude of fine grained regions.

## 2.6 Conductivity

We performed resistivity tests using a four-wire digital multimeter (Agilent Model 34420A Nano Volt/Micro Ohm Meter) per the guidance of ASTM B193 standard [3]. The ends of each of the resistivity specimen were slightly sanded before testing to remove any impurities or oxidation which may have formed on the surface of the specimen. The tests were conducted in an environmental control chamber set at 50% humidity and 20°C in accordance with the ASTM B193 standard. The four-wire or Kelvin method for electrical resistance measurement makes use of an ammeter and a voltmeter to calculate the resistance of a sample without the addition of error from the internal resistance of the data collection wires. By creating two loops, the voltage drop across the main current-carrying wires will not be measured by the voltmeter, and thereby does not factor into the resistance calculation. Furthermore, in the four-wire alligator clips, the jaw halves are insulated from each other at the hinge point, only contacting at the tips where they clasp the subject being measured as shown in Figure 4. Thus, current through the current jaw halves does not go through the voltage jaw halves, and will not create any error-inducing voltage drop along the length of the jaws.

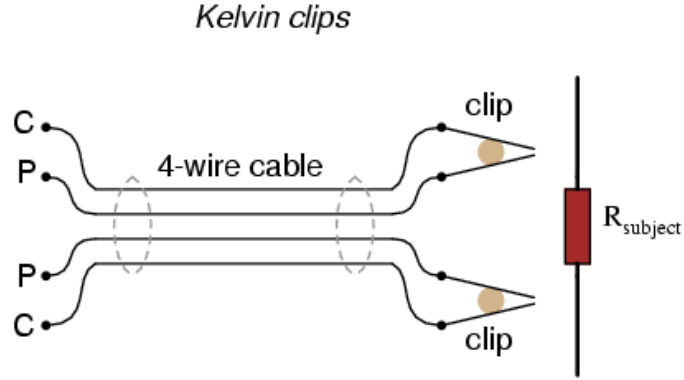


Figure 4: 4-wire resistivity diagram.

The electrical resistivity,  $\rho$ , can be calculated based on the electrical resistance,  $R$ , of the test specimen, the measured cross-sectional area,  $A$ , and the length,  $l$ , of the specimen; as shown in Equation 1.

$$\rho = R \frac{A}{l} \quad [1]$$

Electrical conductivity ( $\sigma$ ) is the inverse of resistivity, as shown in equation 2 .

$$\sigma = \frac{1}{\rho} \quad [2]$$

Conductivity results in specific conductivity per length (S/m) were then divided by the conductivity of annealed pure copper,  $\sigma = 5.8 \times 10^7$  S/m which represents 100 % IACS [4], this ratio yields the % IACS conductivity for each specimen.

Resistivity measurements were taken of 6061 T6, covetic T6, and covetic as-extruded using the process previously discussed. As extruded 6061 was unavailable for resistivity measurements. Using the technique discussed above, resistivity values were converted to conductivity. We had not expected that heat treatment would make a significant difference in electrical conductivity, and had heat treated most of the material, so only a small sample was remaining to perform the measurement in the as-extruded condition. The T6 specimens were approximately 25 cm in length, while the as-extruded specimen was approximately 2.6 cm in length. The dominant term in measurement of conductivity is that of length, so the potential error in the short sample was  $\pm 4.1$  % while the error of the long samples was  $\pm 0.39$  %.

## 2.7 Quasi-static Tensile Testing

We tested standard round tensile specimens of both compositions in the as-extruded condition (processed at 400°F) and in the T6 condition at a constant crosshead speed of 0.025 mm/s. The results are presented in Table 1. In the as-extruded condition the covetic material had a 0.2% offset yield strength of 91.10 MPa (13.2 ksi), about 30% higher than the 68.95 MPa(10.0 ksi) yield strength of the conventional 6061. The fracture edges of the covetic sample were sharp and angular, compared with the conventional 6061 (Figure 6). In the T6 condition there were no substantial differences in tensile properties between conventional and covetic.

Table 1. Tensile test data.

	0.2% YS MPa (ksi)	TS MPa (ksi)	% El.	True Strain to Fracture (%)
6061 As-extruded	68.95 (10.0)	151.68 (22.0)	>20.7*	--
Covetic As-extruded	91.01 (13.2)	155.82 (22.6)	>19.1*	--
6061 T6	273.03 (39.6)	312.33 (45.3)	>18.2*	78
Covetic T6	268.90 (39.0)	306.82 (44.5)	25.1	65

\*Necked outside of gauge marks.

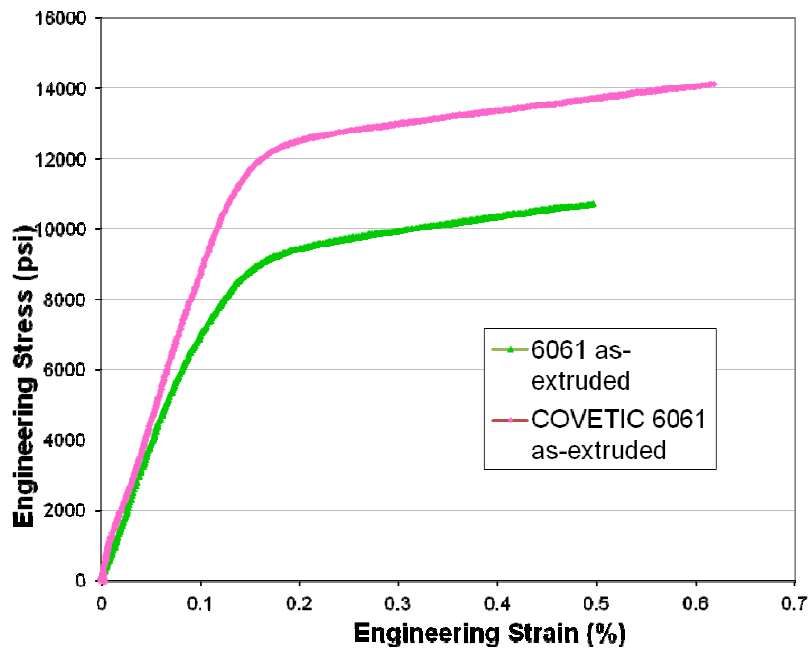


Figure 5: Longitudinal tensile results as-extruded. The yield strength of the covetic material was about 30% higher than that of the conventional 6061.



Figure 6: As-extruded tensile samples. Specimen (a) is 6061 while specimen (b) is covetic. The covetic specimen fracture has a more angular appearance.

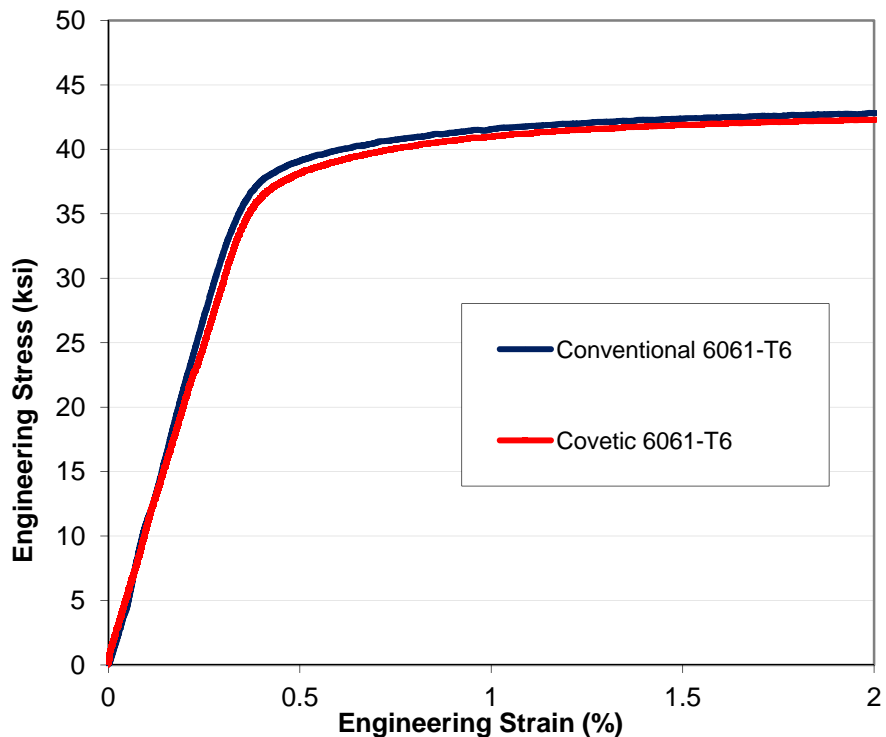


Figure 7: Longitudinal stress-strain curves after T6 heat treatment. There was essentially no difference with or without the nanoscale carbon.

## 2.8 Split Hopkinson Pressure Bar Testing

Strain rate dependency of properties was evaluated for both types of aluminum for comparison purposes, with both specimens heat treated to the T6 condition. High strain rate mechanical testing was conducted using a Split Hopkinson Pressure Bar (SHPB) with four nominal strain rates of 300, 1000, 1500 and 2000  $\text{s}^{-1}$ . Details of SHPB construction, operation, and data analysis may be found in [5]. An annealed C11000 copper pulse shaper of 2 mm thickness and 5 mm diameter was used to obtain an equilibrium stress state in the specimens. The use of pulse

shapers to aid in obtaining the desired stress state is discussed in [6]. Figure 8 presents strain rate plotted on the vertical axis while true strain is plotted on the horizontal axis for the four strain rates. The plateau of the strain rate curve marks an equilibrated stress state within the specimen and thus an average stress can be determined. Figure 9 presents true stress plotted on the vertical axis while true strain is plotted on the horizontal axis for the four nominal strain rates discussed previously. Finally, Figure 10 presents a direct comparison between the 6061-T6 and covetic material at the same strain rate. Note that the data of interest are in the region of plastic deformation. Elastic behavior of the specimen is difficult to capture accurately due to the extremely short time duration of the test, with correspondingly few data points in that regime of material behavior. Data from similar material will rarely align in the elastic regime, as is seen in Figures 9 and 10.

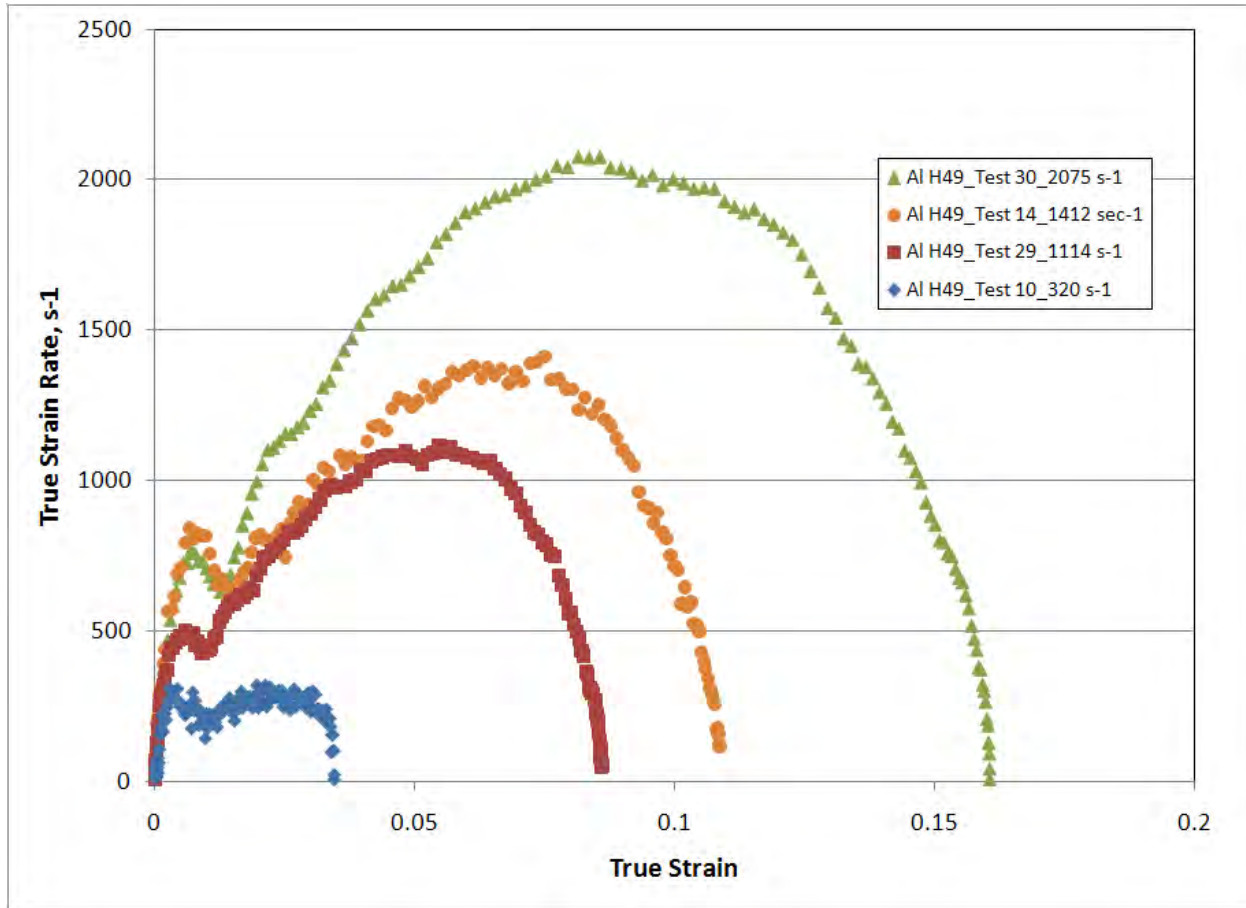


Figure 8: Strain rate plots for covetic aluminum (sample designation H49) heat treated to the T6 condition. Plateau of rate plots marks the equilibrated stress state.

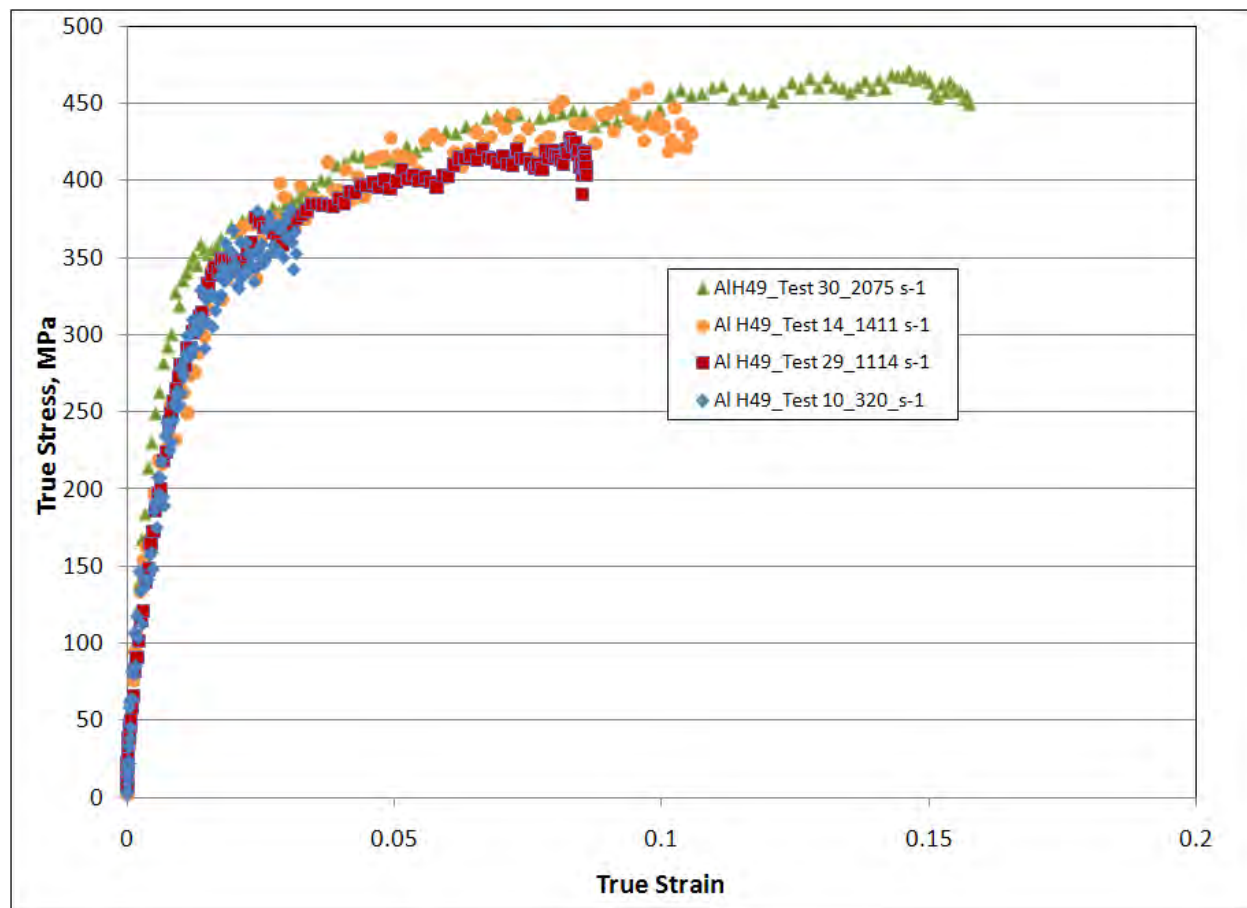


Figure 9: True stress versus true strain for 4 strain rates of covetic aluminum (sample designation H49) heat treated to the T6 condition.

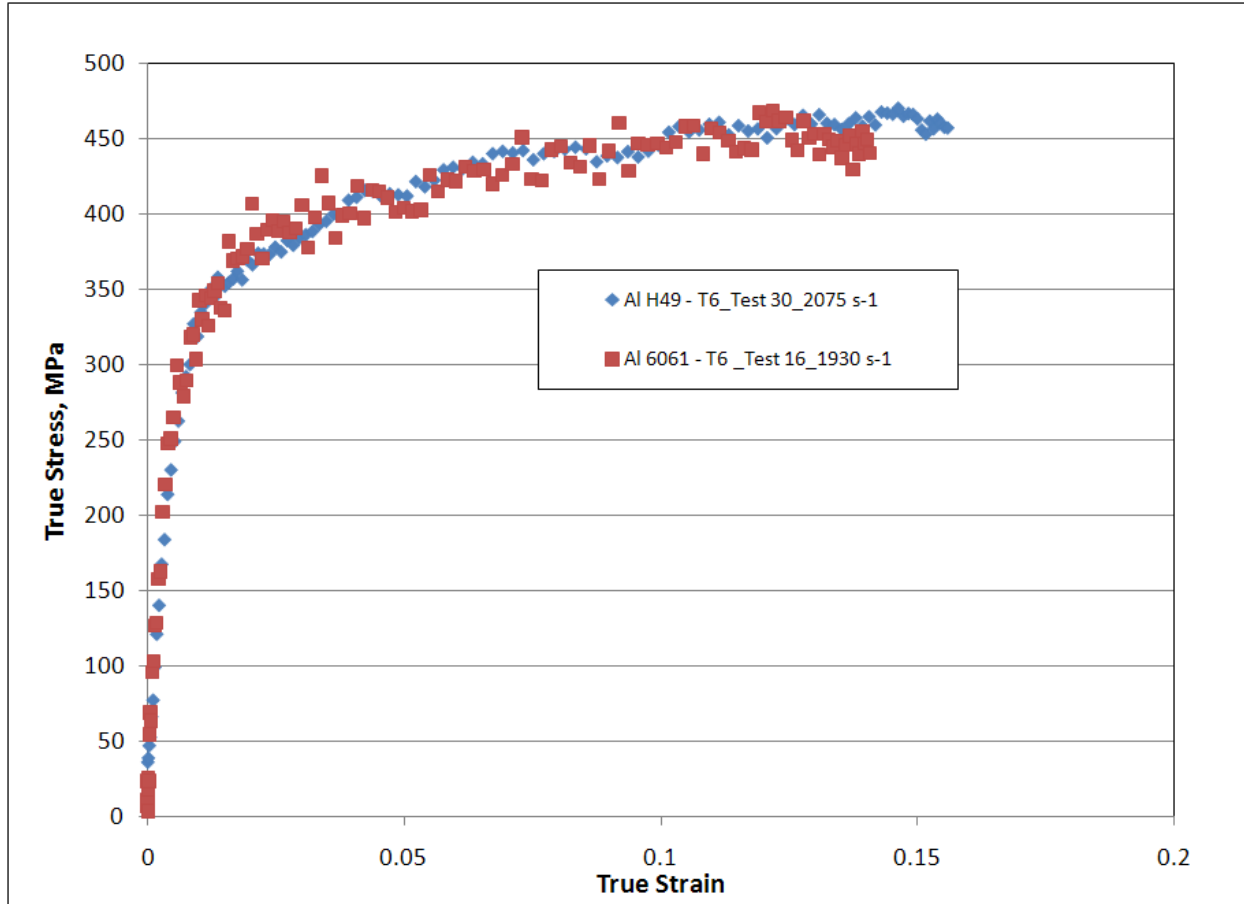


Figure 10: True stress versus true strain for covetic aluminum and 6061 aluminum heat treated to the T6 condition.

## 2.9 Differential Thermal Analysis

A sample of the 3 wt. % covetic AA6061-T6 was sent to Evans Analytical for differential thermal analysis, in order to determine the melting temperature. The solidus temperature of the sample was determined to be 619°C, which is significantly greater than the literature value of 582°C [7]. Except for the presence of nanoscale carbon and unconverted graphite, the material conformed to the chemical specifications for AA6061 in ASTM B211.

## 3. ANALYSIS AND DISCUSSION

The data presented allow a direct comparison between 6061 and covetic aluminum in terms of physical and mechanical properties. Separate discussions are presented in the following sections based on the figures presented earlier.

### 3.1 Density

The determination of density was primarily undertaken to facilitate evaluation of material properties as a function of volume fraction of carbon within the covetic aluminum. Little

difference was noted between the density of 6061 aluminum and that of covetic aluminum. Density of the 6061 aluminum was  $2.678 \text{ g/cm}^3$  while that of the covetic aluminum was  $2.673 \text{ g/cm}^3$ . The small variation in density can be attributed to the low volume percentage of infused carbon, which additionally has a density that is close to that of elemental aluminum.

### 3.2 Rule of Mixtures

A weighted average rule of mixtures can be used to compute the density in particle filled composites. Using the relation shown in Equation 3,

$$\rho_c = V_f \rho_f + (1 - V_f) \rho_m \quad [3]$$

and the handbook values [2] for the density of aluminum,  $\rho_m = \rho_{Al} = 2.678 \text{ g/cm}^3$ , the particle volume fraction,  $V_f$ , can be determined. Density of the added carbon will be an estimate, as the value depends on the structure of the carbon added. For this study, carbon density was estimated to be  $2.25 \text{ g/cm}^3$ , which is the value [2] for the graphitic carbon used in the fabrication of covetic aluminum. Composite density,  $\rho_c$ , is the measured density of the covetic aluminum. Using this technique, carbon volume fraction was estimated to be 1.17%, which is less than one half of the estimated as-manufactured volume fraction of 3.56%.

### 3.3 Hardness and Tensile Strength

For both the 6061 and covetic extruded specimens, the hardness data tended toward higher values as the sample location was translated from sample center to outer edge, as seen in Figure 1. This increase in hardness was attributed to greater work hardening of the outer surfaces of the bulk material as part of the extrusion process. Notice that on average the covetic aluminum was 23.4% harder than the parent 6061 material, with the increase in hardness ranging from as little as 13.2% to as much as 29.2%. This increase in hardness must be attributed to a combination of the presence of the nanocarbon-infused metal, and the warm-working of this structure. The tensile test results showed that heat treating both materials to the T6 condition virtually eliminated strength differences between them, as shown in Table 1. We do not know whether the as-extruded hardness and strength increases were due solely to the finer grain size or to an additional interaction (such as between dislocations and the nanoscale carbon).

### 3.4 Electrical Conductivity

The results are presented in Table 2. Three conductivity specimens were measured; as-extruded 6061 was not available for conductivity tests. In the T6 condition, the covetic material exhibited a conductivity about 1% greater than that of the non-covetic material. This variation was within the error expected of the measurement ( $\pm 3\%$ ).

Table 2. Comparison of Electrical Conductivity of Aluminum Alloys.

Electrical Conductivity Values		
Material	Conductivity, % IACS	Notes
Covetic Aluminum, as-extruded	67.3 ( $\pm 3\%$ )	Test specimen as-extruded at 400°F, before heat treatment
Covetic 6061-T6	47.81 ( $\pm 3\%$ )	Test specimen, extruded+ heat treated to T6
Conventional 6061-T6	47.37 ( $\pm 3\%$ )	Test specimen, extruded+ heat treated to T6
6061-T6	40 – 48	Reference value [2]

Also significant is the change in conductivity of the as-extruded covetic aluminum after heat treatment to a value that closely matches that of conventional 6061 – T6 as shown in lines two and three of Table 2. The measured values are bracketed by the expected range of conductivity shown in line 4 of the table.

### 3.5 Strain Rate Dependency

There was no appreciable difference in strain rate dependent behavior between the two types of aluminum in the T6 condition. Figure 9 demonstrates, regardless of strain rate, that the ultimate compressive stress remains relatively constant for covetic aluminum. Figure 10 provides a direct comparison between the performance of covetic aluminum and its parent material, 6061 aluminum, at the same nominal strain rate of  $2000\text{ s}^{-1}$ . No significant difference in performance is noted between the two alloys. As-extruded condition covetic material and conventional 6061 was unavailable for SHPB testing.

### 3.6 Structure

The fine-grained recrystallized structure throughout the as-extruded covetic material contrasted sharply with the mixture of grain sizes in the conventional material. The coarser randomly oriented grains in the conventional material apparently had grown and coarsened during the elevated temperatures of the extrusion process, probably just after deformation when temperatures are the highest (400°F + an additional excursion due to internal friction during deformation). The covetic material is resistant to grain coarsening and the accompanying loss of strength at this moderately elevated temperature.

## 4. CONCLUSIONS

Our investigations showed that:

- Nanoscale carbon raised the solidus temperature of AA6061 from 582°C to 619°C.
- Nanoscale carbon increased the warm-worked strength and hardness of AA6061 by a factor of 23-30%. When the structure was re-solutionized and aged, the differences disappeared.

- The 6061 covetic aluminum resisted grain coarsening during extrusion, and the finer grain size may have led, at least in part, to the higher strength and hardness as-extruded.
- There was no appreciable difference in strain rate dependent behavior between covetic and conventional 6061 in the T6 condition.
- Nanoscale carbon increased the electrical conductivity of AA6061 from 47.37% to 47.81% IACS which is within the expected error of  $\pm 0.15\%$ .
- As extruded covetic aluminum electrical conductivity was significantly higher than that of 6061 T6 or covetic aluminum that had been re-solutionized and aged.

## 5. ACKNOWLEDGEMENTS

The authors wish to thank the following US Naval Academy personnel for the many efforts exerted on behalf of this research effort. In particular, Mr. Derek Baker and Mr. Matt Stanley were both instrumental to the success of this effort. The contributions of the following at the Naval Surface Warfare Center are gratefully acknowledged: Gregory Archer for the heat treatment and Matthew Hayden for the tensile testing.

## 6. REFERENCES

1. J. Shugart, "New Class of Metallic Nanocomposites," presented at MS&T '09 , Pittsburgh, PA, 25-29 October 2009.
2. MATWEB: Material Property Data, <http://matweb.com>, 2011.
3. ASTM Standard B193, "Standard Test Method for Resistivity of Electrical Conductor Materials," ASTM International, West Conshohocken, PA, 2008.
4. Slade, P. G., ed., Electrical Contacts: Principles and Applications, Boca Raton, CRC Press, 1999, pp 162 – 163.
5. G. Gray, Classic Split-Hopkinson Pressure Bar Testing, ASM Handbook, Vol. 8, H. Kuhn, D. Medlin, Ed., ASM International, Materials Park, Ohio, 2000, pp 462- 476.
6. D. Frew, M. Forrestal, W. Chen, Pulse Shaping Techniques for Testing Brittle Materials with a Split Hopkinson Pressure Bar, Experimental Mechanics, 42, 2002, pp 93 - 106.
7. Metals Handbook, Ninth Edition. v. 2, Properties and Selection: Nonferrous Alloys and Pure Metals, p. 116.